Vibration Sensing for Deployed Metropolitan Fiber Infrastructure

# Vibration Sensing for Deployed Metropolitan Fiber Infrastructure

Ilaria Di Luch[1], Pierpaolo Boffi[1], *Senior Member, IEEE*, Maddalena Ferrario[1], Giuseppe Rizzelli[2], Roberto Gaudino[2], *Senior Member, IEEE*, Mario Martinelli[1], *Member, IEEE*
[1]*Politecnico di Milano, Milan, Italy*, [2]*Politecnico di Torino, Turin, Italy*

***Abstract*—The optical fiber deployed in the metropolitan infrastructure carrying high-speed WDM traffic data is used also for network surveillance, identifying and localizing the onset of vibrations and dynamic stress events, potentially dangerous for the integrity of the fiber telecom asset. A coherent approach is adopted in a counter-propagating interferometer to develop a sensing system exploiting the ring layout of the metro network. With respect to usual dual Mach-Zehnder interferometric sensors, where typically the reference arm is kept isolated, in our arrangement we use as reference arm a fiber inside the same deployed cable, minimizing the impact of the city strong environmental noise. Preliminary assessments of the proposed sensing solution have been experimented in a metro ring of 32-km standard single-mode fiber deployed in the city of Turin, Italy, devoted to telecom applications. The sensor is demonstrated to operate preserving the coexistence with the high-speed WDM telecom traffic. With respect to complex and expensive sensing solutions based on pulsed phase-OTDR techniques, in the present case continuous-wave counter-propagating optical signals are exploited and the spatial resolution in dynamic event localization depends only on the receiver sampling rate: in our implementation, by adopting off-the shelf low-cost commercial 20MS/s sampling boards, 10-meter spatial resolution is experimentally achieved. The proposed sensing solution provides significant added value to the deployed metro fiber infrastructure and the same interferometric approach based on the counter-propagating layout can be easily exploited in metro networks even in case of presence of optical nodes equipped with reconfigurable optical add-drop multiplexers useful for WDM traffic routing**

***Index Terms*—Metro Networks, fiber sensors, interferometric sensors.**

## I. Introduction

NOWADAYS our cities are interconnected by hundreds of kilometers of optical fibers supporting the metropolitan area network (MAN) and the access network. In the next future, it is also estimated the deployment of new deep fiber in the urban infrastructure by the telecom operators and communications service providers, to increase broadband services for residential and business customers, to assure very high-speed access, and to allow wireless densification for 5G. The continuous reinforcement of the metro fiber infrastructure to provide high-speed connections appears mandatory to face the issue of the present digital divide. Actually, the optical fiber running in our cities offers the capability to be used as a pervasive sensor as well, where not only telecom data are carried, but the fiber constitutes the sensitive medium able to detect vibrations, strain, pressure, temperature, etc. This exploitation of the deployed fiber provides an added value to the optical asset itself, allowing a smart monitoring of our cities in a large scale. Recently, a fiber link deployed in the Dallas area, Texas, carrying multi-Tb/s data traffic has been used to monitor vehicle speed and car density in a road [1]. Distributed Acoustic Sensors (DAS) exploiting ocean-bottom fiber optic links has provided seismographic and oceanographic data along a 42 km link with 10-m spatial resolution [2] while distributed vibration patterns along optical communication links were recovered with phase-OTDR technologies [3]. Moreover, deployed passive optical network (PON) infrastructure has been exploited for structural vibration monitoring in smart city applications with the simultaneous downstream of 10-Gb/s NRZ signal [4].

The optical MANs are often organized on ring topologies used, for example, as the primary link of active access networks, where the interconnection between the different network sections takes place through switching devices, e.g. reconfigurable optical add-drop multiplexers (ROADMs) [5]. The ring configuration has the advantage of providing a redundant pathway if a link goes down and is often applied where long distances make difficult to deploy the fiber in a star topology from a central station. The ring layout in the MAN opens the possibility of new sensing applications that can run on a dedicated wavelength in parallel to all the other wavelengths in a dense wavelength division multiplexed (WDM) grid carrying telecom traffic.

In the present work, a coherent sensing system has been exploited on a metropolitan fiber ring, to detect and even localize the onset of vibrations or dynamic stress applied to the fiber link. Indeed, damages or breakages of optical telecommunication infrastructures, due to strong mechanical stress events, caused, for example, by sudden landslides or road works too close to the deployed fiber cable, is a current topical issue that can cause prolonged out of service, requiring time-consuming and high-cost repairs [6]. The proposed diagnostic solution, embedded in the metro ring can thus provide a real-time monitoring of the structural health of the optical cable itself and also of the surrounding environment.

Experimental demonstration to assess the performance of such a sensing system is presented for a deployed 32-km ring cable of standard single-mode fiber (SSMF) running in the city of Turin, Italy, devoted to telecommunication applications. The sensing system proposed in this work exploits the capabilities of a coherent approach [7] combined to a dual Mach-Zehnder interferometer (MZI) arranged in a loop configuration. The use of a counter-propagating layout allows the localization of the dynamic events. A similar scheme was previously considered

This article has been accepted for publication in a future issue of this journal, but has not been fully edited. Content may change prior to final publication. Citation information: DOI 10.1109/JLT.2021.3051732, Journal of Lightwave Technology



by the Authors [8] but, in that case, a local oscillator was exploited and system performance, in terms of localization accuracy and maximum monitorable fiber ring length, were severely affected by the laser source coherence and relative phase noise. In the present case instead, exploiting two fibers available inside the deployed cable, both sensing and reference signals of each MZI could run in parallel along the same path length, as suggested in [9], thus making the solution almost independent from the coherence of the exploited laser source. Moreover, being reference and sensing fibers paired in the same cable, this drastically reduced the common mode phase noise caused by the city environment, whose entity would otherwise have prevented any vibration detection. Indeed, with respect to [9], the main purpose of this work is to prove the feasibility of a dual MZ scheme in a real-noisy-environment for the detection of impulsive events on the optical link.

The experimented sensing system, relying on the detection of counter-propagating continuous wave optical signals and implemented with off-the-shelf low-cost optoelectronic devices and digital acquisition boards, provides a simple and reliable solution for optical network surveillance, able to identify in advance potentially dangerous situations that can affect the integrity of the optical metro link, without resorting to more complex and expensive pulsed-based phase-OTDR (Optical Time Domain Reflectometer) distributed solutions [1]–[3], [10], [11].

The paper is organized as follows. After the introduction in Section I, Section II shows the theoretical algorithm useful for the localization of a vibration or a stress event in a distributed interferometric sensor arranged in a loop configuration, where two counter-propagating clockwise (CW) and counterclockwise (CCW) optical signals travel along the same deployed optical cable. Moreover, the demodulation algorithm used to convert the phase shift induced by the dynamic event into an intensity change is briefly presented for the dual MZI scheme employed in our sensor, exploiting two symmetrical 3x3 optical couplers as coherent receivers [7]. In Section III the experimental layout is detailed while in Section IV experimental results are described, discussing the impact of the environmental noise due to the urban deployment and the adopted solution to minimize its impairment. Moreover, performance in terms of spatial accuracy in the localization of dynamic event is evaluated by comparing different post-processing algorithms applied to measured phase time signals. Also the coexistence with WDM data transmission is shown, demonstrating negligible impact of the sensing signals copropagating in the ring with telecom traffic. Finally, in Section V the implementation of the proposed sensing system in MAN ring also in presence of network nodes equipped with reconfigurable optical add-drop multiplexers (ROADMs) able to route the WDM traffic is discussed, followed by the Conclusions in Section VI.

## II. Signal Processing for Vibration Localization

### A. Localization algorithm

The proposed sensing system based on a coherent approach exploits a distributed interferometric layout arranged in a loop configuration in order to perform the event localization: the continuous light from a laser source travels along the same fiber in two counter-propagating directions, CW and CCW, that is clockwise and counterclockwise respectively. If a vibration affects the fiber, a phase modulation $\Delta\phi(t)$ is induced in both CW and CCW optical signals. The localization process then simply relies on the evaluation of the time of arrival difference $\Delta T$ between the two counter-propagating phase modulations $\Delta\phi(t)$.

As shown in Fig.1, if $L$ is the total length of the fiber ring and an event occurs at an arbitrary point $z = Z_P$, the two modulated phases will travel:

$$\begin{aligned} L_{CW} &= L - Z_P \\ L_{CCW} &= Z_P \end{aligned} \tag{1}$$

for the clockwise and counterclockwise direction respectively. The two phase modulations $\Delta\phi_{CW}$ and $\Delta\phi_{CCW}$ have a Time-of-arrival $\Delta$T which can be derived as follow:

$$\Delta T = \frac{L - Z_P}{\upsilon}, \tag{2}$$

where $\upsilon$ is the light velocity in the medium. The position $Z_P$ is easily retrieved from (2) as:

$$Z_P = \frac{L - \Delta T \cdot \upsilon}{2}. \tag{3}$$

As the two counter propagating lights are emitted by the same laser source and have been affected by the same impulsive event, the two received phases signals result strongly correlated and can be written as follow:

$$\Delta\phi_{CW} = S(t) + n_1(t), \tag{4}$$

$$\Delta\phi_{CCW} = S(t - \Delta T) + n_2(t), \tag{5}$$

where $S(t)$ is the interference signal induced in the fiber by the event, $n_1(t)$ and $n_2(t)$ are the additional noise signals which accumulate progressively along the propagation in the fiber ring and which can be modelled as mutually independent random processes, as in [9]. These noise contributions, for the present application, are mainly caused by the city environment and accumulate progressively along the propagation in the fiber ring. A further source of noise can be also introduced by the optical source coherence in presence of possible imbalances between the sensing and reference arms. In the real application, phase signals are sampled and digitalized in order to be post-processed and analyzed. The sampling process imposes a fixed estimation error since, typically, the time delay

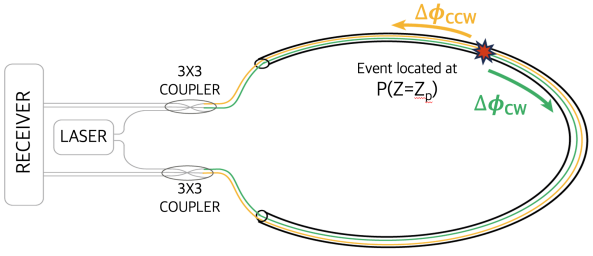


Fig. 1: Set up of a dual MZI, comprising two 3x3 couplers

This article has been accepted for publication in a future issue of this journal, but has not been fully edited. Content may change prior to final publication. Citation information: DOI 10.1109/JLT.2021.3051732, Journal of Lightwave Technology



is not a integer multiple of the sampling interval. Eq. (3) can be thus modified and the localization estimation becomes:

$$Z_P = \frac{L - N \cdot T_s \cdot \upsilon}{2}, \tag{6}$$

where $N$ is the integer number of samples of delay between the two phases $\Delta\phi_{CW}$ and $\Delta\phi_{CCW}$ and $T_s$ is the sampling interval. Thus, the system spatial resolution $R_s$in event localization results:

$$R_s = \upsilon \cdot T_s. \tag{7}$$

while the resulting theoretically accuracy in the estimation of $\Delta$T, and thus of $Z_P$, is $\pm T_s$. In practice, however, this accuracy results degraded by phase noise contributions mentioned above. Objective of this work is to provide an effective assessment of the localization accuracy of the proposed coherent solution exploited in a real noisy environment.

### B. Demodulation Algorithm

The two counter-propagating phase signals $\Delta\phi_{CW}$ and $\Delta\phi_{CCW}$, are separately retrieve by means of two independent coherent receivers, each one exploiting a 3x3 optical coupler coherent demodulator as explained in [12], [13] and shown in Fig.2. The following explanation, referred to $\Delta\phi_{CCW}$, likewise applies to $\Delta\phi_{CW}$.

The 3x3 coupler performs a passive stable homodyne demodulation where the output signals are 120° phase shifted and the corresponding receiver photocurrents can be written as:

$$\begin{aligned} I_1 &= C + B\cos(\Delta\phi(t)_{CCW} - 2/3\pi), \\ I_2 &= C + B\cos(\Delta\phi(t)_{CCW} + 2/3\pi), \end{aligned} \tag{8}$$

where $\Delta\phi(t)_{CCW}$ is the phase difference induced by the dynamic event between the CCW sensing and reference arms of the ring interferometer. $C$ and $B$ are constants that depend on the coupling coefficient $k_{ij}$ of the 3x3 coupler as:

$$\begin{aligned} B &= 2\sqrt{k_{12}k_{13}k_{22}k_{32}}, \\ C &= 2k_{11}k_{22} + k_{13}k_{32}. \end{aligned} \tag{9}$$

Finally, to retrieve the phase difference $\Delta\phi(t)_{CCW}$, $I_1$ and $I_2$ can be processed to retrieved the following sum and difference:

$$\begin{aligned} I_{cos} &= I_1 + I_2 = \cos(\Delta\phi(t)_{CCW}), \\ I_{sin} &= I_1 - I_2 = \sin(\Delta\phi(t)_{CCW}). \end{aligned} \tag{10}$$

From Eq.(10) calculating the arc-tangent of the ratio between $I_{sin}$ and $I_{cos}$, and the $\Delta\phi(t)_{CCW}$ is obtained:

$$\Delta\phi(t)_{CCW} = \text{atan}\frac{I_{\sin}}{I_{\cos}} = \text{atan}\frac{\sin(\Delta\phi(t)_{CCW})}{\cos(\Delta\phi(t)_{CCW})}. \tag{11}$$

Thanks to the adopted coherent demodulation scheme, based on a 3x3 coupler, the phase signal $\Delta\phi(t)_{CCW}$ can be retrieved in a completely passive way without the need of an active feedback for quadrature point stabilization as in conventional fiber optic interferometry. Yet, with respect to the Michelson scheme adopted in [7], [13], the present MZ ring layout works in transmission and signal polarization cannot be retraced by exploiting Faraday rotator mirrors. However, the noise caused by the city environment rapidly scrambles the polarization of both reference and sensing signals intrinsically avoiding any polarization fading issues in $\Delta\phi(t)_{CCW}$ recovery.

## III. Experimental Layout

To experimentally assess the proposed sensing system in a real deployed network, we exploited a 32-km SMF ring deployed in the city of Turin, Italy, belonging to one of the Italian FTTH operators (Fig.2-right) in order to prove the feasibility of metro fiber infrastructure for sensing purposes, e.g. for monitoring the structural integrity of the fiber itself. The dual MZI is thus arranged in a loop configuration as shown in Fig.2-left, where counter-propagating CW and CCW optical signals travel along two fibers inside the same deployed optical cable [14]. The two fibers act as the sensing and reference arm of each Mach-Zehnder interferometer. The continuous light emitted by a laser source (linewidth $\Delta\nu = 100kHz$) is split by a 50:50 coupler and enters the two symmetric 3x3 couplers. Two ports of each 3x3 coupler are connected to the sensing and reference fibers of the MZ ring. After propagation, each pair of signals travelling into the ring (two for the CW and two for the CCW directions) interfere and are coherently demodulated in the other 3x3 coupler at the end of their path. The four

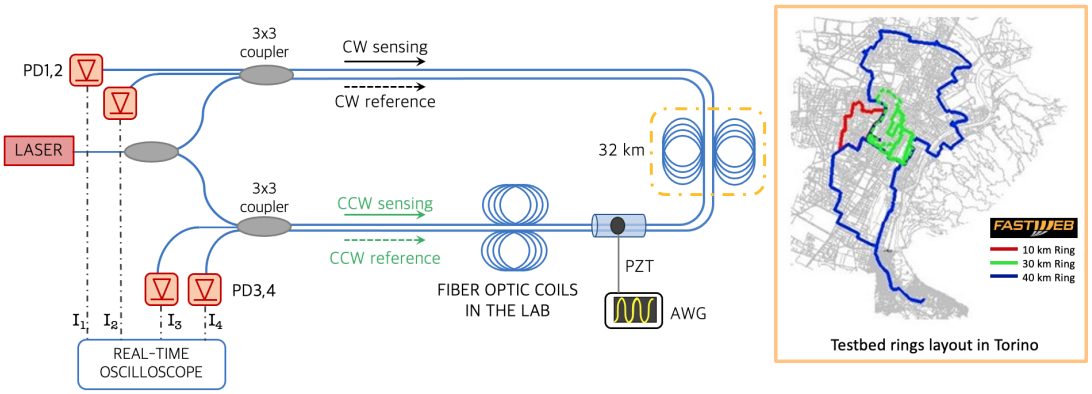


Fig. 2: Experimental layout (on the left) comprising a 32 km fiber ring deployed in the city of Turin (on the right)

This article has been accepted for publication in a future issue of this journal, but has not been fully edited. Content may change prior to final publication. Citation information: DOI 10.1109/JLT.2021.3051732, Journal of Lightwave Technology



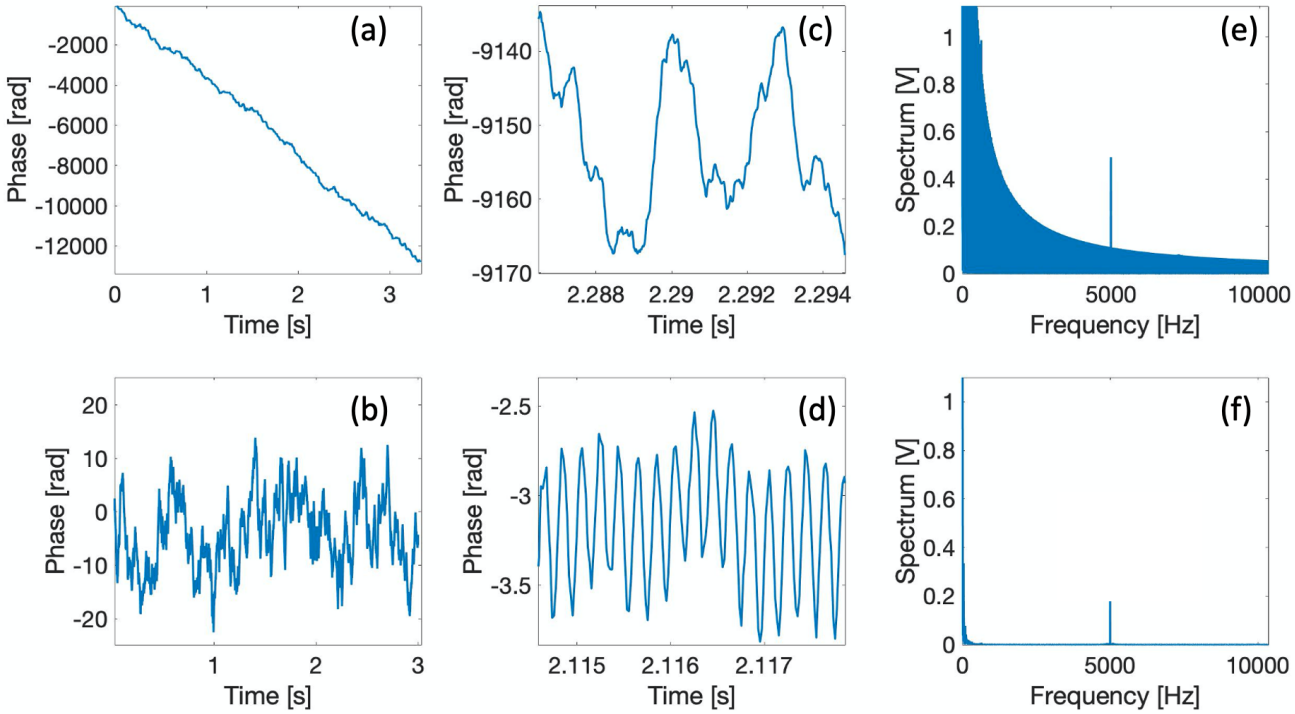


Fig. 3: Examples of recovered phase signals in case of a) reference fiber inside the lab, b) paired fibers along the ring. Detailed of the temporal behavior of 5kHz vibration in the case of c) reference fiber inside the lab, d) paired fiber along the ring. Corresponding frequency spectra in case of e) reference fiber inside the lab, f) paired fibers along the ring.

optical signals are simultaneously detected by 125 MHz photoreceivers (NEP $= 25\,\mathrm{pW}/\sqrt{\mathrm{Hz}}$), sampled by a 20MS/s real-time oscilloscope board (4 channels Picoscope 5442D with 13 bit) and post-processed, as detailed in the previous paragraph, to recover $\Delta\phi_{CW}$ and $\Delta\phi_{CCW}$ and evaluate the relative time delay $\Delta T$ for vibration localization [8], [14]. In particular, $\Delta\phi_{CW}$ and $\Delta\phi_{CCW}$ are separately retrieved by means of coherent receivers constituted by a simple 3x3 optical coupler providing the in-phase I and quadrature Q components of each interferometric signal [13]. Although the frequency band of mechanical and acoustic vibrations is in the order of kHz, a 20MS/s sampling rate is required to guarantee a 10-meter spatial resolution in event localization. We believe this is a good tradeoff between a reduced DSP complexity (20 MS/s can today be implemented on extremely cheap programmable electronic boards) and a spatial accuracy in fault location that is more than adequate for metro network.

## IV. Vibration Monitoring Characterization and Experimental Results

### A. Environmental Noise Suppression

As stated before, the two counter-propagating phases signals $\Delta\phi_{CW}$ and $\Delta\phi_{CCW}$ have to be correlated to perform their relative time delay estimation. The correlation is more accurate the more the phase noise affecting $\Delta\phi_{CW}$ and $\Delta\phi_{CCW}$ is low. As mentioned before, noise contributions are mainly due to the two laser sources coherence and to the city environment. With respect to the former one, the optical source phase noise can be modelled as a random walk noise with a variance that depends on the ratio between the laser coherence length $\ell_c$ and the path unbalance $\Delta L$ between the two arms of the interferometer. As long as $\Delta L$ is kept much lower than $\ell_c$, that is:

$$\Delta L < \ell_c = \frac{c}{\pi \Delta\nu}. \tag{12}$$

where $\Delta\nu$ is the laser linewidth, the laser phase noise contribution does not affect the accuracy in the recovery of $\Delta\phi$. The rule of thumb is to guarantee a path difference $\Delta L$ not exceeding one tenth of the coherence length, in order to ensure measurements with a good Signal to Noise Ratio (SNR) [8]. To minimize instead the latter noise contribution, that is, the one caused by the city environment, which progressively accumulates along the fiber ring, the idea was to exploit the availability of two fibers paired inside the deployed cable. Typically, interferometric sensors have their reference arm kept separated from the measurement area [8], [14]. to guarantee the highest sensitivity. In the case under test, however, as phase noise contributions caused by the city environment are significantly strong, the reference and sensing arms were chosen along the same path. In this way, the common mode noise is reduced, at the expense, of course, of a reduction of the actual detected vibration signal. To prove the feasibility of this solution it was initially verified the possibility of detecting a vibration tone generated by a PZT on the fiber to emulate a dynamic stress event. In particular, a $900\mu m$ tight fiber cable was wrapped for 1.5m length around the cylindrical piezo-transducer (PZT) and a 5kHz sinusoidal signal with an amplitude of 14V was applied to the PZT, inducing a dynamic deformation of about $160n\epsilon$ on the fiber, corresponding to a

This article has been accepted for publication in a future issue of this journal, but has not been fully edited. Content may change prior to final publication. Citation information: DOI 10.1109/JLT.2021.3051732, Journal of Lightwave Technology



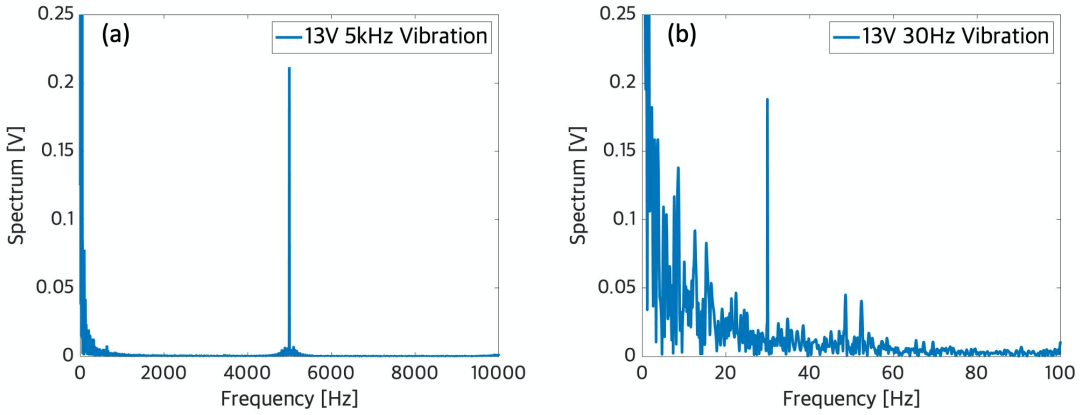


Fig. 4: Frequency spectra for a) 5kHz and b) 25 Hz applied vibrations with paired fiber along the link.

sinusoidal tone signal with a $\Delta\phi_{pk-pk} = 1rad$. Fig.3 shows the time behaviour and the spectral content of the recovered phase signal $\Delta\phi$ for the case of a 32 km reference fiber kept inside the lab compared to the configuration depicted in Fig.2 with reference and sensing fibers paired in the same cable. It can be seen from Fig.3-a how in the former case the phase noise increases by 12000 radians in just a few seconds; moreover, both Fig.3-c and the spectral content in Fig.3-e show a strong noise contribution up to frequencies of the order of kHz: the 5kHz vibration can still be detected with a 7 dB SNR but the detection of lower PZT-induced vibrations is prevented. Measurements reported in Fig.3-(d-f) highlight instead how the use of paired fibers inside the deployed cable drastically reduces to only a few tens of radians the integral noise accumulated along the link, while, at the same time, the slight difference in the geometric arrangement of the fibers on the PZT is sufficient to allow to reveal the vibration signal with an improved SNR of 20dB.

The analysis was also extended to lower frequencies that are more representative of real mechanical vibrations. An example is reported in new Fig.4 were a 25Hz signal (14 V amplitude) was applied to the PZT in the case of paired fibers. Fig.4 clearly shows that, even with fibers coupled in the same cable, environmental noise is not fully compensated below 100Hz and the SNR starts to degrade, reducing to 10dB at 25Hz. For even lower frequencies, [0-20]Hz range, a same SNR can be guaranteed if the strain on the fiber cable is of the order of at least $1\mu\epsilon$.

### B. Impulsive Event Localization

Afterwards, by exploiting the two coherent systems coupled in the counter-propagating configuration of Fig.2 we verified the possibility of localizing an impulsive dynamic event emulating an intrusion or a sudden damage. Initially, different coil lengths, namely of 100 m, 1 km and 4.5 km were connected to one side of the deployed ring network and an impulsive event was generated with the PZT attached near the junction. The PZT was excited with 80V square pulses and $450\mu s$ which in turn caused a natural damping response of the PZT itself. Fig.5-(a-b) shows the corresponding recovered signals $\Delta\phi_{CW}$ and $\Delta\phi_{CCW}$ measured for the case of a 1km coil attached to the ring network, resulting in a delay $\Delta T = 153.3\ \mu$s in agreement with a $\Delta L = 31km$ (fiber refractive index n=1.483). We then proceeded by adding a 4.5 km fiber coil to the fiber ring and by placing the PZT after the coil. Fig.5-(c-d) shows the corresponding recovered signals $\Delta\phi_{CW}$ and $\Delta\phi_{CCW}$ where, in this case, the resulting delay of $\Delta T = 136.1\ \mu s$ corresponds to an estimated $\Delta L = 27.5km$. Repeated measurements confirmed a promising accuracy of $\pm 15m$ of the proposed approach in dynamic event localization as will be detailed in the next paragraph.

As cleary visible in Fig.5, the PZT response has a known and repeatable shape, featuring a sharp wavefront, which makes the identification of the event easier even in presence of strong noise. We thus decided to perform further measurements in order to validate the localization technique even for realistic intrusion event. We generated a perturbation by manually hitting the floor under which the optical cable passed before entering the laboratory. The acquired signals $\Delta\phi_{CW}$ and $\Delta\phi_{CCW}$, shown in Fig.6, still feature an impulsive wavefront caused by the pressure waves impacting on the fibers inside the deployed cable. This has allowed to estimate a time delay $\Delta T = 158.2\ \mu s$ in agreement with a $\Delta L = 32km$, having hit the cable at the end of the metro ring. Accuracy in vibration localization will be discussed in the following paragraph, comparing performance obtained for PZT-induced and manually intrusive signals in dependence of different applied post-processing algorithms for $\Delta L$ estimation.

### C. Accuracy Assessment

Time delay evaluation represents the key point for vibration localization and, in this work, two different approaches have been taken into account and compared to assess the one providing the best performance in terms of localization accuracy. As stated in Sec.II-B the two counter-propagating phases $\Delta\phi_{CW}$ and $\Delta\phi_{CCW}$ are strongly correlated, however, the presence of the residual environmental noise can be affected the correct estimation of their relative time delay. The first approach relies on the cross correlation of the two phase signals and on the evaluation of the resulting cross-correlation peak. As stated in [15], [16], the observation time $T_{obs}$ to be selected to calculate the correlation depends on the maximum

This article has been accepted for publication in a future issue of this journal, but has not been fully edited. Content may change prior to final publication. Citation information: DOI 10.1109/JLT.2021.3051732, Journal of Lightwave Technology



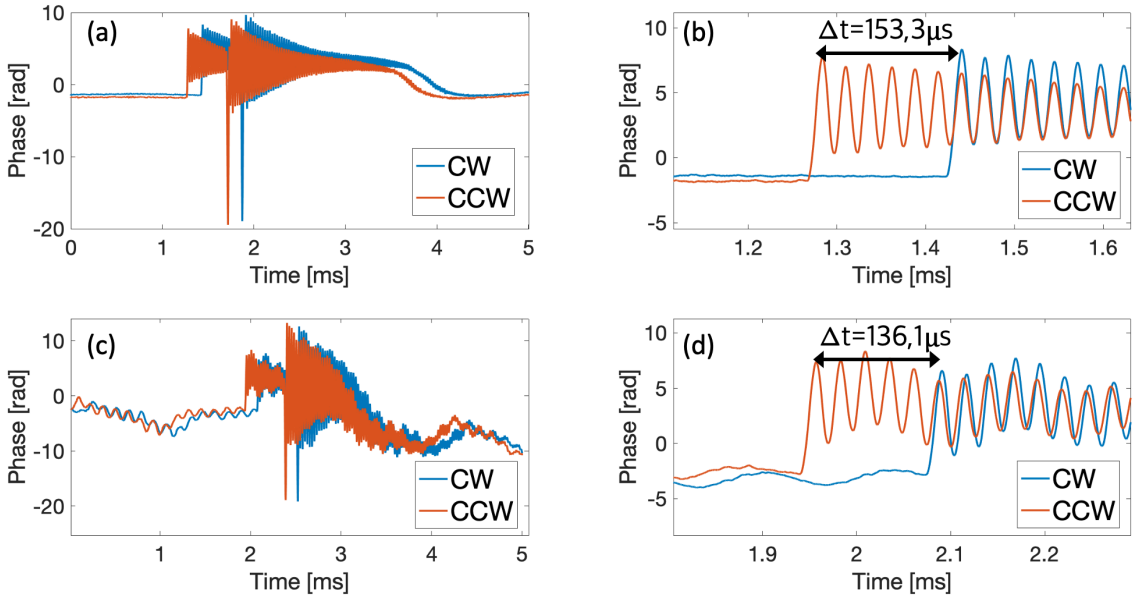


Fig. 5: Recovered $\Delta\phi_{CW}$ and $\Delta\phi_{CCW}$ phase signals generated by a PZT impulse applied after 1km (a) and after 4.5 km (c) fiber coil attached to the 32 km fiber ring network. Detail of the onset of the detected impulsive event generated by a PZT after 1km (b) and after 4.5 km (d) fiber coil.

frequency $f_{max}$ of the signal spectral content, that is, on its bandwidth $W$, according to :

$$f_{max} \cdot T_{obs} = W \cdot T_{obs} >> 1 \tag{13}$$

To verify Eq.13, the original traces of $10^5$ samples at 20MS/s ($T_{obs} = 5ms$) were therefore progressively windowed to perform correlation, respectively, on 1/10, 1/50 and 1/100 of the recorded trace length. This processing has been applied both PZT signals and manually hit signals. Of these latter ones both raw signals and low-pass filtered signals were analized and compared. Estimated accuracy resulting over 20 repeated measurements for each case are reported in Table.I. It can be noticed, in general, that cross correlation provides good results for PZT signals while, in the case of the manually hit signals, that do not feature sharp wavefronts and are thus more affected by environmental noise, a pre-filtering of the signal is required. Pre-filtering is performed by smoothing the two phase signals $\Delta\phi_{CW}$ and $\Delta\phi_{CCW}$ with a moving average algorithm that leads to an accuracy improvements from $\pm 55m$ to $\pm 25m$ in the case of the cross-correlation applied to the whole signal trace and from $\pm 45m$ to $\pm 20m$ for the correlation over 1/10 of the trace. From Table.I it is also evident that only 1/100 of the whole trace is too short to perform a correct and reliable delay estimation for both PZT and manually hit signals. Indeed, having the PZT a damping frequency of 38 kHz, with $T_{obs} = 0.05ms$ (i.e. 1/100 window) Eq.13 is no more satisfied. Same considerations holds for the manually hit signals that also feature spectral components up to kHz. The second approach that has been considered in this work, as an alternative to cross correlation, rely on the estimation of the first maximum (Max picking) of the two phase signals and on the evaluation of their relative time delay.

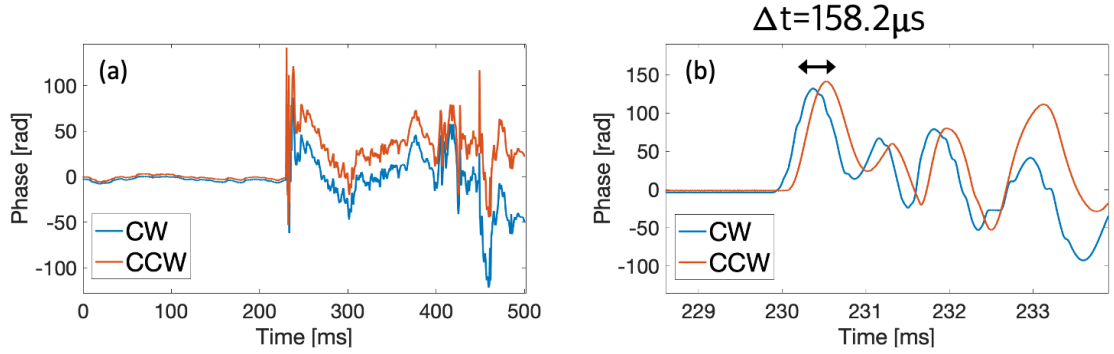


Fig. 6: a) Recovered $\Delta\phi_{CW}$ and $\Delta\phi_{CCW}$ signals in case of manual impulsive event on 32 km fiber ring network. b) Detail of the onset of the detected impulsive event.

This article has been accepted for publication in a future issue of this journal, but has not been fully edited. Content may change prior to final publication. Citation information: DOI 10.1109/JLT.2021.3051732, Journal of Lightwave Technology



TABLE I: Methods Evaluation

| Signal Types | | Estimation Method Accuracy [m] | | | |
|---|---|---|---|---|---|
| | | Xcorr | Xcorr 1/10 Windowed | Xcorr 1/100 Windowed | Max |
| PZT | | ± 17 | ± 17 | ± 35 | ± 15 |
| Hit | Raw | ± 55 | ± 45 | ± 82 | ± 38 |
| | Filtered | ± 25 | ± 20 | ± 65 | ± 15 |

Table.I shows that better results can be achieved with this method, which also benefits from signal pre-filtering. In case of manually hit signals the accuracy, in fact, improves from $\pm 38m$ to $\pm 15m$ by applying the moving average filter. Results reported in Table I and evaluation carried out thus confirm that the maximum-picking method, combined to signal pre-filtering, is a simple yet effective method that can guarantee a good accuracy of $\pm 15m$ in impulsive event localization along real metro optical networks.

### *D. Simultaneous Sensing and Data Transmission*

The same set up shown in Fig.2 has been arranged to simultaneously perform vibration monitoring and wavelength division multiplexed (WDM) data transmission. At the transmission side a 2x2 optical coupler (with 3dB loss) was used to couple the narrow continuous wave optical source at 1550 nm (FWHM 100 kHz) used for sensing purposes with a downstream 10Gb/s NRZ signal generated by an externally modulated tunable external cavity laser (ECL) (P=0dBm) onto the two fibers of the ring. The overall ring features 10dB losses. At the receiver side an erbium doped fiber amplifier (EDFA) with 15 dB gain was used to amplify the incoming signal and a C-band 40-channel WDM multiplexer was used to separate the two signals and filter the EDFA ASE noise. Two adjacent WDM bands with a 50 GHz spacing were used for the sensing signal and the modulated data. The WDM channel of 12.5 GHz bandwidth has about 9 dB insertion loss, bringing the overall link loss up to 22dB. The sensing signal, always kept below +5dBm in order not to induce non-linear effects, was detected by a PIN photodiode with -35dBm sensitivity, enough to manage the all the link losses.

Instead, the data carrying signal was also detected through a PIN photodiode and the resulting electrical waveform acquired through a real-time oscilloscope with 33 GHz bandwidth and 100 GHz sampling frequency. The bit error rate (BER) was then computed through offline digital signal processing (DSP) including clock recovery and simple feed forward equalization. The impact of the sensing signal on transmission performance has been evaluated by measuring the sensitivity curves as a function of the received optical power, varied at the receiver input by means of a variable optical attenuator (VOA). Results are reported in Fig.7.

No significant detrimental effect of the sensing system can be observed on the performance of the transmission system at the considered power levels of the interfering CW sensing signal. The sensitivity curves overlap almost perfectly, with small discrepancies only for BER values close to the error free limit ($3.2 \cdot 10^{-5}$ in our case with 30707 processed bits).

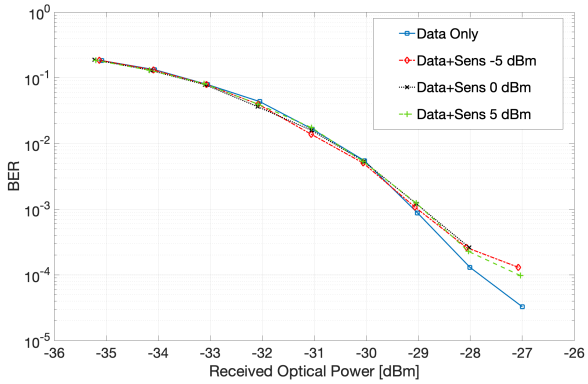


Fig. 7: BER vs. received signal power $P_{RX}$, after 32 km, for different power levels $P_{IN}$ of the interfering sensing signal.

## V. Discussion for the Implementation in a ROADM-based Ring Network

The proposed sensing solution, thanks to its ring topology and typical operation distances over tens of kilometers, is potentially suitable for modern metro ring networks, where distributed monitoring would be particularly interesting for early detection of anomalous conditions, that can induce damages or breakages of the fiber infrastructure. The experimental solution that is the focus of our paper, as described in Fig.2, uses anyway the two ring fibers in a bidirectional way. On the contrary, today reconfigurable optical add-drop multiplexer (ROADM)-based dense wavelength-division multiplexed (DWDM) ring metro networks employ isolators in the optical amplifiers making each fiber path strictly mono-directional [5], [17]. To apply the same experimented sensing architecture, four mono-directional fiber paths are thus required, as shown in Fig.8, exploiting two pairs of sensing and reference fibers (one pair for clockwise and one for counterclockwise propagation). The architecture in Fig.8 would dedicate to sensing only one wavelength (in each of the four paths), leaving all the other wavelengths in the used DWDM comb available for the normal data traffic transmission and routing inside the metro ring. In this way no additional components (such as couplers/splitters) are necessary in the link to split a part of the signals for sensing applications and no extra losses are introduced. Hence, the proposed sensing solution does not impact on the infrastructure (also when it is already installed) and on the overall power budget of the telecom channels.

## VI. Conclusion

We proposed an interferometric sensing architectures exploiting the installed metropolitan fiber network for the monitoring of vibrations and the detection of the onset of dynamic stress events that may damage and put out of service the optical infrastructure. All the sensing monitoring is achieved preserving the coexistence with the high-speed telecom data traffic transmission. Preliminary assessments of the proposed

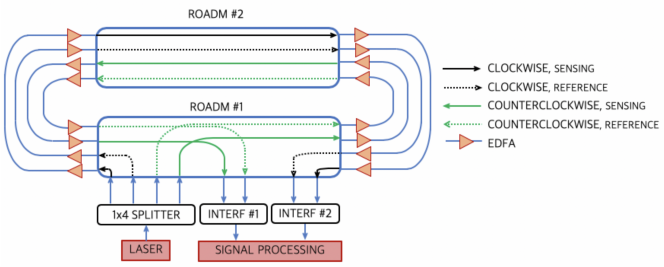


Fig. 8: Extension of the proposed architecture in a ROADM-based ring network.

sensing solutions have been experimented by exploiting the metro fiber link deployed in the city of Turin. The spatial resolution in the event localization depends on the adopted sampling rate at the receiver: a 10-meter spatial resolution has been demonstrated with off-the-shelf programmable 20MS/s sampling boards, without the necessity of complex and expensive sensors, such as phase-OTDR. The proposed sensing solutions provide significant added value to the present and future installed metro fiber infrastructure, that can turn into simple and reliable embedded systems for optical surveillance, preventing dangerous damages to both urban buildings and the optical network infrastructure itself, offering unprecedented potential to provide a fruitful synergy between telecommunications and sensing applications.

## REFERENCES

[1] G. A. Wellbrock, T. J. Xia, M.-F. Huang, Y. Chen, M. Salemi, Y.-K. Huang, P. Ji, E. Ip, and T. Wang, "First field trial of sensing vehicle speed, density, and road conditions by using fiber carrying high speed data," in *Optical Fiber Communication Conference Postdeadline Papers 2019*. Optical Society of America, 2019, p. Th4C.7.

[2] E. Williams, M. R. Fernández-Ruiz, R. Magalhães, R. Vanthillo, Z. Zhan, M. Gonzalez-Herraez, and H. Martins, "Distributed sensing of microseisms and teleseisms with submarine dark fibers," *Nature Communications*, vol. 10, p. 5778, 12 2019.

[3] P. Jousset, T. Reinsch, T. Ryberg, H. Blanck, A. Clarke, R. Aghayev, G. Hersir, J. Henninges, M. Weber, and C. Krawczyk, "Dynamic strain determination using fibre-optic cables allows imaging of seismological and structural features," *Nature Communications*, vol. 9, 12 2018.

[4] I. D. Luch, M. Ferrario, G. Rizzelli, R. Gaudino, and P. Boffi, "Vibration sensing for deployed metropolitan fiber infrastructures," in *Optical Fiber Communication Conference (OFC) 2020*. Optical Society of America, 2020, p. Th3F.6.

[5] Jörg-Peter Elbers and Klaus Grobe, "Optical metro networks 2.0," in *Optical Metro Networks and Short-Haul Systems II*, W. Weiershausen, B. Dingel, A. K. Dutta, and A. K. Srivastava, Eds., vol. 7621, International Society for Optics and Photonics. SPIE, 2010, pp. 47 – 58.

[6] G. Maier, A. Pattavina, S. Patre, and M. Martinelli, "Optical network survivability: Protection techniques in the WDM layer," *Photonic Network Communication*, vol. 4, 01 2003.

[7] M. Martinelli and M. Ferrario, "Synoptic fiber optic sensor," patent No. WO 2013/179118 Al, Published Dec. 5th., 2013.

[8] J. Morosi, M. Mattarei, M. Ferrario, P. Boffi, and M. Martinelli, "Coherent fiber-optic sensor for vibration localization," in *2014 Fotonica AEIT Italian Conference on Photonics Technologies*, 2014, pp. 1–4.

[9] Q. Sun, D. Liu, J. Wang, and H. Liu, "Distributed fiber-optic vibration sensor using a ring mach-zehnder interferometer," *Optics Communications*, vol. 281, no. 6, pp. 1538 – 1544, 2008.

[10] Y. Shi, H. Feng, and Z. Zeng, "A long distance phase-sensitive optical time domain reflectometer with simple structure and high locating accuracy," *Sensors (Basel, Switzerland)*, vol. 15, pp. 21 957–21 970, 09 2015.

[11] R. Zinsou, X. Liu, Y. Wang, J. Zhang, Y. Wang, and B. Jin, "Recent progress in the performance enhancement of phase-sensitive OTDR vibration sensing systems," *Sensors (Basel, Switzerland)*, vol. 19, no. 7, April 2019.

[12] P. Boffi, G. Cattaneo, L. Amoriello, A. Barberis, G. Bucca, M. F. Bocciolone, A. Collina, and M. Martinelli, "Optical fiber sensors to measure collector performance in the pantograph-catenary interaction," *IEEE Sensors Journal*, vol. 9, no. 6, pp. 635–640, 2009.

[13] C. Sbarufatti, L. Martinelli, M. Mattarei, M. Ferrario, and M. Giglio, "Ultrasonic strain wave acquisition by a low-cost fiber optic coherent sensor for structural health monitoring applications," 2016.

[14] X. Liu, B. Jin, Q. Bai, Y. Wang, D. Wang, and Y. Wang, "Distributed fiber-optic sensors for vibration detection," *Sensors*, vol. 16, p. 1164, 07 2016.

[15] J. Ianniello, "Time delay estimation via cross-correlation in the presence of large estimation errors," *IEEE Transactions on Acoustics, Speech, and Signal Processing*, vol. 30, no. 6, pp. 998–1003, 1982.

[16] A. Kumar and Y. Bar-Shalom, "Time-domain analysis of cross correlation for time delay estimation with an autocorrelated signal," *IEEE Transactions on Signal Processing*, vol. 41, no. 4, pp. 1664–1668, 1993.

[17] S. Sarmiento, J. A. Altabas, D. Izquierdo, I. Garces, S. Spadaro, and J. A. Lazaro, "Cost-effective DWDM ROADM design for flexible sustainable optical metro–access networks," *IEEE/OSA Journal of Optical Communications and Networking*, vol. 9, no. 12, pp. 1116–1124, 2017.